

Mechanism of Growth of the Ge Wetting Layer Upon Exposure of Si(100)-2 × 1 to GeH₄

Chie-Sheng Liu, Li-Wei Chou, Lu-Sheng Hong,* and Jyh-Chiang Jiang*

Department of Chemical Engineering, National Taiwan University of Science and Technology,
43, Keelung Road, Section 4, Taipei, 106, Taiwan

Received December 4, 2007; E-mail: hongls@mail.ntust.edu.tw; jcjiang@mail.ntust.edu.tw

Germanium (Ge) semiconductor materials receive much attention because of their unusual optoelectronic properties and their compatibility with well-established silicon (Si) technologies.¹ Ultrahigh vacuum chemical vapor deposition (UHV-CVD) is the technique employed most often to fabricate Ge/Si heterostructures. Understanding the mechanism of these surface reactions is, therefore, vitally important for developing such heteroepitaxial growth systems; in this case, the Stranski–Krastanow (S–K) mode dominates the growth of Ge on the Si surface.² Initial studies of the surface reactions of the hydrides silane (SiH₄) and germane (GeH₄) were aimed predominantly at determining the adsorption states or understanding the mechanisms of hydrogen desorption from the surfaces.^{3,4} After dissociative adsorption, however, unraveling the mechanisms through which the adsorbed Ge atoms become incorporated into the lattice—completing the film growth process—has remained a challenge.

In consideration of the reaction pathways for lattice incorporation after dissociative adsorption, Kang and Musgrave⁵ reported that the energy barrier for the opening of a Si dimer after dissociative adsorption of SiH₄ was as high as 70 kcal/mol, much larger than the barrier for hydrogen desorption^{3,4} in the CVD process. Although the presence of radicals would lower the barrier for cleavage of the dimer bond,⁵ such species are rarely produced in conventional thermal CVD processes without the use of a hot filament. To determine the underlying reaction kinetics that occur after dissociative adsorption, in this study we performed UHV-CVD experiments and theoretical calculations to investigate the mechanism of formation of the initial Ge wetting layer on Si(100)-2 × 1 reacted with the molecular hydride GeH₄.

In this Communication, we report the initial reaction kinetics for Ge deposition after exposing a Si(100)-2 × 1 surface to GeH₄ in a UHV-CVD system. The growth rate of Ge, especially at the wetting layer stage, was investigated using in situ X-ray photoelectron spectroscopy (XPS) to measure the signals for Ge atoms at the onset of deposition. We used experimental growth rate data obtained at temperatures ranging from 698 to 823 K to determine, for the first time, the activation energy for the growth of the Ge wetting layer from GeH₄ on Si(100)-2 × 1. We also performed density functional theory (DFT) calculations to explore the possible surface reaction pathways. We established two-dimer (Si₃₁H₃₂) and three-dimer (Si₄₅H₄₄) cluster models and monitored their reactions with GeH₄. With these cluster models, we found that one hydrogen atom of an adsorbed species GeH₃(a) migrated to the neighboring dimer, causing the Ge-appended Si dimer bond to break more readily. The Ge atom then became incorporated into the lattice after ring closure.

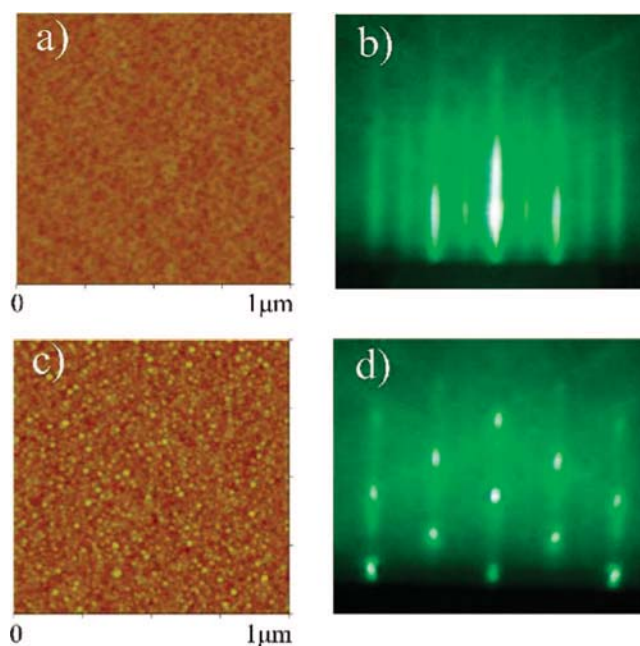


Figure 1. Images of Ge grown from GeH₄ on Si(100)-2 × 1 at 723 K in a UHV-CVD apparatus: (a) AFM image and (b) RHEED pattern after 20-min deposition; (c) AFM image and (d) RHEED pattern after 25-min deposition.

Figure 1 panels a and c display tapping-mode atomic force microscopy (AFM) images recorded after 20- and 25-min depositions, respectively, of GeH₄ at 723 K in the UHV-CVD apparatus; Figure 1 panels b and d present the corresponding reflection high-energy electron diffraction (RHEED) patterns of the AFM images. After 25-min deposition, dots appeared in the AFM image and spotty 1 × 1 patterns appeared in the RHEED pattern; in contrast, after 20-min deposition the surface images displayed a smooth morphology and streaky 2 × 1 lines, respectively. These results indicate that Ge deposition under these conditions obeys the S–K growth mode.

To understand the reaction kinetics underlying the growth of the flat wetting layer, we performed a target exploration (Figure 2) using in situ XPS to record the signals of the Ge 2p_{3/2} orbital, which provides a larger amount of surface information because of the high surface sensitivity of its photoelectrons. Figure 2a displays the Ge 2p_{3/2} spectra obtained for the samples deposited at 723 K as a function of deposition time. The Ge 2p_{3/2} signals were clearly observable when the deposition time was less than 20 min, indicating that layer-by-layer growth of Ge must have occurred on Si(100) because

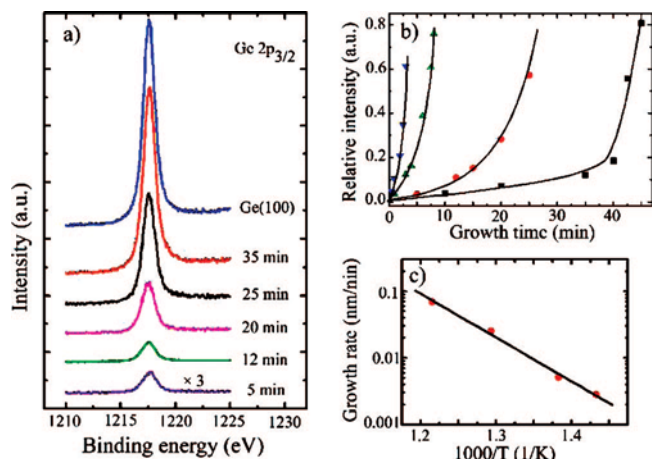


Figure 2. Analysis of growth kinetics for Ge deposition from GeH_4 onto $\text{Si}(100)\text{-}2 \times 1$: (a) XPS $\text{Ge } 2p_{3/2}$ spectra recorded after deposition at 723 K; (b) normalized intensities of Ge deposited at (■) 698, (●) 723, (▲) 773, and (▼) 823 K; the lines are provided only to guide the reader's eye; (c) Arrhenius plot based on growth rate data for the deposition of a 0.2-ML Ge film.

Figure 1a revealed that the surface retained its smooth morphology. Figure 2b presents the normalized integrated photoelectron intensities of the $\text{Ge } 2p_{3/2}$ signals recorded for the samples deposited at temperatures within the range 698–823 K. The slopes of curves increased slightly during the initial phase, but increased dramatically thereafter. We attribute this phenomenon to the transition from layer-by-layer growth to island growth occurring at a critical layer thickness, which we calculated according to the Beer–Lambert law⁶ to be ca. 2 monolayers (MLs). Because we were interested in the mechanism of the process occurring at the very beginning of the Ge wetting layer growth on the $\text{Si}(100)\text{-}2 \times 1$ surface, we determined the growth rate at the point of ca. 0.2-ML Ge deposition by dividing the film thickness by the deposition time at various deposition temperatures (Figure 2c). We observed a precise Arrhenius temperature dependence at the onset of growth of the Ge wetting

layer and calculated the activation energy to be 30.7 kcal/mol for a 0.2-ML Ge coverage at temperatures ranging from 698 to 823 K.

An activation energy of 30.7 kcal/mol at the very beginning of the growth of the Ge wetting layer cannot be attributed to the reaction controlled by hydrogen desorption from the surface because the active sites become apparent after preheating the surface at 1100 K; nevertheless, the barrier for hydrogen desorption from a Ge surface⁴ (33 kcal/mol) is close to our calculated barrier. In contrast, the chemisorption barriers of hydrides^{3–5} are generally much lower than this governing activation energy.

With increasing Ge coverage to near 1 ML, the experimentally determined activation energy exhibited surface coverage dependence (Figures S1 and S2, Supporting Information). That is, the activation energy decreased to 19.1 kcal/mol when the surface coverage increased to 1 ML. The variation of the activation energy with respect to the surface coverage indicates that a series of complex surface reactions prevails during the heterogeneous transformation of the $\text{Si}(100)\text{-}2 \times 1$ surface to a Ge surface. Similar phenomena have been reported for the reaction probability measurement of Ge hydrides on Si surfaces,⁷ for Si film growth from SiH_4 on $\text{Si}(100)$,³ and for deuterium desorption from Ge-covered $\text{Si}(100)$ surfaces,⁸ where H or Ge coverage might affect the kinetic process. Herein, as a first step toward determining the full mechanism, we propose a possible mechanism—based on the following quantum chemistry calculations—for the reaction occurring at the onset of Ge deposition.

To investigate the reaction of GeH_4 on a $\text{Si}(100)$ surface, we employed a cluster model $\text{Si}_{31}\text{H}_{32}$ comprising two dimers to represent a bare $\text{Si}(100)\text{-}2 \times 1$ surface. In this cluster model, unphysical dangling bonds of silicon atoms, except for those on the surface, were terminated with hydrogen atoms. Figure 3 presents the energy level diagram for the reaction of a GeH_4 molecule on a bare $\text{Si}(100)$ surface, evaluated at the UB3LYP/6-31G* level of theory. We considered three reaction steps for the adsorption of GeH_4

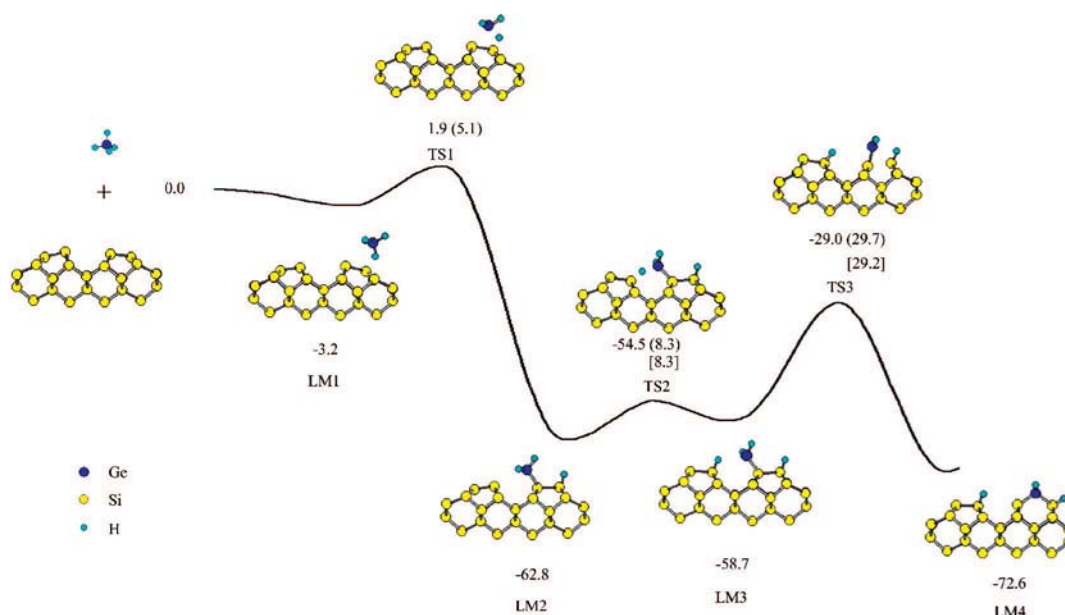


Figure 3. Reaction path for the deposition of GeH_4 on a $\text{Si}(100)\text{-}2 \times 1$ surface. Energies are provided in kcal/mol; values in parentheses and brackets represent energy barriers calculated using the two- and three-dimer clusters, respectively.

on Si(100). In the first step (LM1 to LM2), the molecule dissociated into germanium trihydride and a hydrogen atom ($\text{GeH}_3 + \text{H}$) and adsorbed onto a Si dimer site through a process that was exothermic by 62.8 kcal/mol. The calculated energy barrier was 5.1 kcal/mol, which is quite consistent with the reported values for chemisorptions from hydrides.^{3–5} In the second step (LM2 to LM3), the hindered rotation of $\text{GeH}_3(\text{a})$ along the Ge–Si bond leads one hydrogen atom on $\text{GeH}_3(\text{a})$ to migrate to the neighboring dimer through a process having an energy barrier of 8.3 kcal/mol. The third step (LM3 to LM4) is bond cleavage of the Si dimer bearing the GeH_2 and H units, occurring with an energy barrier of 29.7 kcal/mol, and bridging of the Si dimer atoms through a GeH_2 group. The dimer bond cleavage and the bridging of the $\text{GeH}_2(\text{a})$ unit to the Si dimer are critical aspects of the Ge atom being incorporated into the lattice to complete the Ge film growth. Prior to opening of the dimer, H atom migration to the neighboring dimer appears to assist in lowering the energy barrier for cleavage of the Si–Si bond. With this cluster model, the energy barrier for opening the Si dimer bond with GeH_4 is lower than that for a one-dimer cluster model with SiH_4 .⁵ Moreover, the energy barrier for this process of dimer opening is comparable with the activation energy we obtained experimentally (30.7 kcal/mol) at ca. 0.2 ML. This result suggests that Si dimer opening should be the rate-determining step at the onset of growth of the Ge wetting layer from GeH_4 on the $\text{Si}(100)\text{-}2 \times 1$ surface.

Additional calculations using larger cluster models—up to the three-dimer cluster $\text{Si}_{45}\text{H}_{44}$ —provided very similar results (Figure 3; see Figures S3–S8 and Tables S1–S5 in the Supporting Information for a comparison of the structural parameters and energies of the calculated two- and three-dimer clusters). The calculated energy barrier for Si dimer opening in the three-dimer cluster was lower than that in the two-dimer cluster by only 0.5 kcal/mol, confirming the accuracy of the proposed reaction models.

Although the subsequent mechanism occurring after bridging of the $\text{GeH}_2(\text{a})$ unit to the Si dimer remains unclear, our reaction model revealed the formation of some active sites, that is, radicals (Figure S9, Supporting Information), after dimer bond cleavage and bridging of the $\text{GeH}_2(\text{a})$ unit to the Si dimer. These active sites on the $\text{Si}(100)\text{-}2 \times 1$ surface might lower the energy barrier for further Ge incorporation—possibly one of the reasons why the activation energy decreased with increasing Ge coverage (see Figures S2 and the detailed discussion provided in the Supporting Information).

In summary, we have used XPS, RHEED, and AFM surface analysis techniques to study the mechanism occurring

at the onset of Ge deposition during the decomposition of GeH_4 on $\text{Si}(100)\text{-}2 \times 1$ in a UHV-CVD system and, complementarily, deduced the reaction mechanism through a series of quantum chemistry calculations. A kinetic study concerning the growth of the wetting layer revealed an activation energy of 30.7 kcal/mol for a ca. 0.2-ML Ge coverage. This governing energy barrier correlates well with the results of DFT calculations, which suggested that opening of the Si dimer following a H atom migration would be the rate-controlling step for the initial growth of the Ge wetting layer on $\text{Si}(100)\text{-}2 \times 1$ from GeH_4 . In addition, two- and three-dimer cluster models provided us with extra dimer units with which to model the H atom migration from $\text{GeH}_3(\text{a})$ to an open site; this process assists the system to overcome the energy barrier for the opening of the Si dimer bond. We hope that the experimental and theoretical results reported herein will be of use in understanding the mechanism of layer growth on Si substrates.

Acknowledgment. We thank the National Science Council of Taiwan for supporting this research financially (NSC 94-2214-E-011-005 and 95-2113-M-011-001). We are grateful to the National Center for High-Performance Computing for computer time and facilities.

Supporting Information Available: Experimental details; theoretical calculation methods; detailed discussion of the subsequent reaction mechanism; detailed structural parameters and energies calculated from the two- and three-dimer clusters. This material is available free of charge via the Internet at <http://pubs.acs.org>.

References

- (1) (a) Dadykin, A. A.; Naumovets, A. G.; Kozyrev, Yu. N.; Rubezhanska, M. Yu.; Lytvyn, P. M.; Litvin, Yu. M. *Prog. Surf. Sci.* **2003**, *74*, 305. (b) Colace, L.; Balbi, M.; Masini, G.; Assanto, G.; Luan, H.-C.; Kimerling, L. C. *Appl. Phys. Lett.* **2006**, *88*, 101–111.
- (2) (a) Eaglesham, D. J.; Cerullo, M. *Phys. Rev. Lett.* **1990**, *64*, 1943. (b) Medeiros-Ribeiro, G.; Bratkovski, A. M.; Kamins, T. I.; Ohlberg, D. A. A.; Williams, R. S. *Science* **1998**, *279*, 353.
- (3) (a) Liehr, M.; Greenlief, C. M.; Kasi, S. R.; Offenberger, M. *Appl. Phys. Lett.* **1990**, *56*, 629. (b) Eres, G.; Sharp, J. W. *J. Appl. Phys.* **1993**, *74*, 7241. (c) Greenlief, C. M.; Liehr, M. *Appl. Phys. Lett.* **1994**, *64*, 601. (d) Rauscher, H. *Surf. Sci. Rep.* **2001**, *42*, 207. (e) Satake, K.; Graves, D. B. *J. Chem. Phys.* **2003**, *118*, 6503.
- (4) Cunningham, B.; Chu, J. O.; Akbar, S. *Appl. Phys. Lett.* **1991**, *59*, 3574.
- (5) Kang, J. K.; Musgrave, C. B. *Phys. Rev. B* **2001**, *64*, 245–330.
- (6) Vickerman, J. C. *Surface Analysis—The Principle Techniques*; Wiley: New York, 1997; Chapter 3, p 60.
- (7) Lam, A. M.; Zheng, Y.-J.; Engstrom, J. R. *Surf. Sci.* **1997**, *393*, 205.
- (8) (a) Ning, B. M. H.; Crowell, J. E. *Appl. Phys. Lett.* **1992**, *60*, 2914. (b) Ning, B. M. H.; Crowell, J. E. *Surf. Sci.* **1993**, *295*, 79. (c) Kim, H.; Taylor, N.; Abelson, J. R.; Greene, J. E. *J. Appl. Phys.* **1997**, *82*, 6062. (d) Kim, H.; Taylor, N.; Bramblett, T. R.; Greene, J. E. *J. Appl. Phys.* **1998**, *84*, 6372.

JA710802S